DOI: http://doi.org/10.4038/jgssl.v22i2.68 *Journal of Geological Society of Sri Lanka Vol. 22-2 (2021), 57-65*

POTENTIAL APPLICATION OF BUTTALA IRON ORES FOR THE SYNTHESIS OF HEMATITE NANOPARTICLES

V.G.C. SAMANMALI[1], T.B.N.S. MADUGALLA[2] *, H.A.K.L. MANJULA [1]

[1]*Department of Chemical Sciences, Faculty of Applied Sciences, South Eastern University of Sri Lanka, Sammanthurai, Sri Lanka*
[2]*Department of Physical Sciences, Faculty of Applied Sciences, South Eastern University of Sri Lanka, Sammanthurai, Sri Lanka*

**Corresponding author e-mail: nadeeshamadugalla@seu.ac.lk*

(Received 17th August 2021; accepted 2nd December 2021)

ABSTRACT

Hematite nanoparticles (HNPs) are widely used in present-day industries owing to their remarkable properties. In this study, the potential use of the iron ores of Buttala, Sri Lanka was investigated as a source of iron for the synthesis of HNPs. Initially, the mineralogy and the chemistry of the Buttala iron ores were analyzed using X-Ray Diffractometer (XRD) and X-Ray Fluorescence analyzer (XRF) respectively. For the synthesis of HNPs, representative powdered fractions of the raw iron ores were acid digested and the recovered ferric ions were used as the iron precursor. The HNPs were synthesized by using the co-precipitation method and polyethylene glycol was used to prevent agglomeration. The yielded product was mineralogically and morphologically characterized with XRD and Scanning Electron Microscope (SEM). The mineralogical results indicated that the raw iron ores are mainly composed of magnetite, hematite and goethite with minor spinel and ilmenite while the XRF analyses revealed that they contain high amount of Fe_2O_3 (77.80%) and low concentrations of Al_2O_3, SiO_2, MgO, and TiO_2. The acid-insoluble residue contains spinel, ilmenite, and quartz indicating the complete dissolution of hematite, magnetite, and goethite during the digestion. The XRD analyses coupled with SEM images of the synthesized product revealed that the product is hematite representing both spherical and irregular thin flaky morphologies. The size of these particles ranges from 90 to 130 nm and the calculated yield of synthesized HNPs is 92.57%. Therefore, the Buttala iron ores can potentially be used as a source of iron for the production of HNPs.

Keywords: *Hematite nanoparticles, Buttala iron ore deposit, Co-precipitation, XRD, SEM.*

1. INTRODUCTION

Value-addition to raw material is an essential contributor to the growth of a nation (Dissanayake et al., 2019). Among the available industrial mineral deposits in Sri Lanka, iron ores have greater economic potential since they can be used as raw materials to synthesis iron-based nanoparticles such as Hematite nanoparticles (HNPs), magnetite nanoparticles and maghemite nanoparticles etc. (Dissanayake et al., 2019; Jalil et al., 2019). Of these iron-based nanoparticles, the HNPs are widely used in many industries such as Gas sensors (Chen et al., 2005; Yang et al., 2011), catalysts (Lin and chen 2014; Yasuhara and Hochella, 2019), magnetic recording materials (Wu et al., 2010; Tadic et al., 2014), fine ceramics (Francis et al., 2010), pigments (Müller et al., 2015; Sultan et al., 2016), and photoelectrochemical cells (Wang et al., 2002; Meng et al., 2013).

The HNPs can be synthesized using various methods including (i) solvothermal (Lu *et al.*, 2006), (ii) sol-gel (Opuchovic and Kareiva, 2015), (iii) gas-phase deposition methods (Wheeler et al., 2012), (iv) thermal oxidation and pyrolysis approaches (Wheeler et al., 2012), (v) hydrothermal (Tang et al., 2006), (vi) electrochemical methods (Wheeler et al., 2012) and (vii) co-precipitation (Lassoued et al., 2017). In these methods, the size and the shape of the compounds can be changed depending on some parameters, such as the duration, temperature, pH, ionic strength, concentration and type of the surfactant, and the nature of the iron salts

(Schwertmann et al., 1999; Chen et al., 2017; Lassoued et al., 2017). Of these methods, the co-precipitation is more attractive due to its low cost, high purity, short preparation time, high homogeneity and relatively low reaction temperature (Liu et al., 2005; Liu et al., 2008; Hua et al., 2009). Naturally available, iron ore tailing, iron-rich soil, and iron ores can be used as iron precursors to synthesize HNPs by applying these methods (Dissanayake et al., 2019; Jalil et al., 2019).

The high-grade basement of Sri Lanka is composed of a number of iron ore deposits and they are classified into three broad groups: (i) magnetite deposits, (ii) copper-magnetite deposits, and (iii) hydrated iron oxide deposits [Fig. 1 (Cooray, 1984; Herath, 1995; Jayawardena, 1984)]. Nearly two decades ago, an additional iron ore deposit has been discovered in Buttala, Monaragala District, closer to the lithotectonic boundary between the Highland Complex (HC) and the Vijayan Complex (VC) [Fig. 1 (Amarasekara et al., 2014; Hewathilake et al., 2013; Senaratne et al., 2001)]. The deposit is exposed as a small mountain covering about 550,000 m^2 of surface area and composed mostly of magnetite and hematite with a higher concentration of Fe (Avg. 78.84 wt. %) and lesser gangue elements accommodating easy mining and extraction processes (Hewathilake et al., 2013; Manjula and Madugalla, 2018; Manjula et al., 2020). Therefore, these deposits could be easily utilized as a source material for the preparation of HNPs. The present study aims to investigate the potential use of Buttala ore deposit to synthesis HNPs.

Of the three types of iron ore deposits found in Sri Lanka, the hydrated iron ore deposits are commonly found in the southwest part of the country, mainly in Ratnapura district and in a few localities in Galle and Matara districts (Jayawardana et al., 2014). These are near surface, smaller, scattered bodies of highly ferruginous laterite deposits, rich in iron hydroxides mainly of goethite and limonite with average Fe content of 55 % (Cooray, 1984; Fernando, 1986; Herath, 1995; Jayawardena, 1984; Jayawardana et al., 2014). Among the hydrated deposits in the country, the deposits in Dela, Noragolla, Opata and Poronuwa in Ratnapura district and Wilpita in Galle district are economically important (Fernando, 1986; Herath, 1995; Jayawardena, 1984). The copper-magnetite type deposits exposed in Seruwila village in Trincomalee district near the boundary between the Highland Complex and the Vijayan Complex are mainly composed of magnetite, chalcopyrite, pyrrhotite and pyrite with several gangue minerals including scapolite, apatite, tremolite, diopside and hornblende (Herath, 1995). Although these deposits contain more than 4 million tons of reserves with 1 to 2 % copper and 40 % metallic iron, the deposits occur 100 m below the surface limiting the economical open cast mining (Fernando, 1986). Several primary magnetite type iron ore deposits are exposed at Wilagedara in Sandalankawa, Panirendawa in Chilaw and Kukurampola in Buttala (Jayawardena, 1984; Senaratne et al., 2001). In addition to them, small occurrences of magnetite deposits are found in Mooloya Estate, Hewaheta and Karametiya (Herath, 1995). However due to the small tonnage, grade, depth and discontinuous nature, the magnetite deposits at Panirendawa and Wilagedara are considered uneconomical.

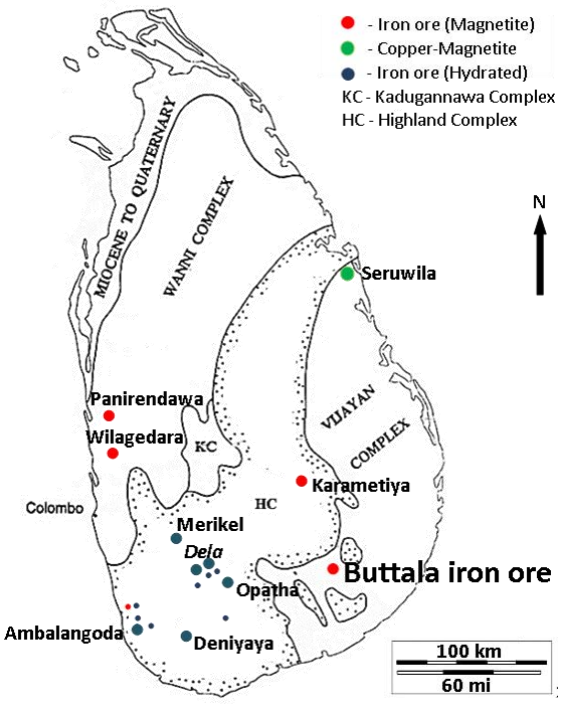

Fig. 1: *A map showing the spatial distribution of iron ore deposits in Sri Lanka*

2. MATERIALS AND METHODS

2.1 Materials

Analytical grade polyethylene glycol 6000 (PEG), NaOH pellets (≥98%, anhydrous) and HCl (37%) were purchased from Sigma-Aldrich. Iron ore samples collected from the Buttala deposit were used as the iron precursor for the synthesis of HNPs. The samples were initially mineralogically and texturally investigated to obtain the un-weathered pure samples (Fig. 2a). Then the samples were cleaned using distilled water, dried and crushed. Finally, representative fractions of crushed samples were sieved to obtain particles less than 150 μm (Fig. 2b). These sieved fractions were used to study the chemical and mineralogical characteristics of the raw iron ores as well as to synthesis of HNPs.

2.2 Characterization of raw iron ores

The chemical characterization was carried out using Rigaku NEX type Wavelength Dispersive X-Ray Fluorescence spectrometer (WD-XRF) available at Gem and Jewellery Research and Training Institute (GJRTI), Kaduwela, Sri Lanka and the mineralogical characterization was done by the Bruker D8 advanced Eco X-Ray Diffraction System (XRD) available at Postgraduate Institute of Science (PGIS), University of Peradeniya, Sri Lanka.

2.3 Preparation of HNPs

Summary of chemical preparation of HNPs is shown in Fig. 3. For the chemical synthesis of HNPs, the powdered representative fractions of iron ores were acid digested using concentrated HCl (11.55 M) for 2 hours under 80 ºC to leach out the iron content and to remove other mineral impurities. The acid insoluble residue (AIR) was separated and then dried to use in further characterizations. The mineralogy of AIR was investigated using the XRD available at PGIS, University of Peradeniya. The yielded light brown filtrate ($FeCl_3$) after the acid digestion was used as the Fe precursor for HNP preparations. Initially, PEG 6000 and 1.5 M NaOH were added drop wise to the diluted $FeCl_3$ simultaneously over a period of 1 hour at 70 ºC with continuous stirring until reddish-brown colour suspension was formed. The PEG 6000 was used as the surfactant to prevent the agglomeration of synthesized nanoparticles (Panda et al., 2009; Díaz et al., 2016). At pH ~11.0, a dark colour HNP suspension was formed. After cooling to room temperature (28 ˚C), the HNPs were centrifuged at 3000 rpm for 15 minutes. Then the supernatant was removed and HNPs crude was dried in an oven at 70 ºC for 2 hours to obtain a dry HNPs (Fig. 2c).

2.4 Characterization of synthesized HNPs

The yielded HNPs were mineralogically and morphologically characterized by using XRD available at PGIS, University of Peradeniya, and Hitachi SU6600 Scanning Electron Microscope (SEM) analyzer available at the Sri Lankan Institute of Nanotechnology (SLINTEC) in Homagama, Sri Lanka respectively.

3. RESULTS AND DISCUSSION

3.1 Mineral and chemical characteristics of raw iron ores

The mineralogical analysis based on the XRD showed the presence of characteristic peaks for iron-bearing minerals of magnetite, goethite and hematite. In addition to that, characteristic peaks for the spinel ($MgAl_2O_4$) and ilmenite ($FeTiO_3$) appear as low-intensity peaks or overlapped

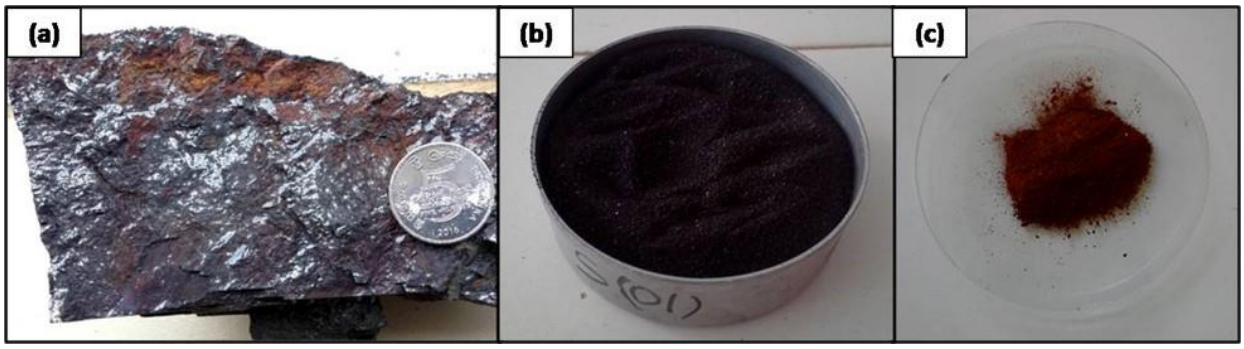

Fig. 2: *Photos showing; (a) magnetite rich Buttala iron ore samples; (b) powdered iron ores and (c) the resulted powder of HNPs during the process*

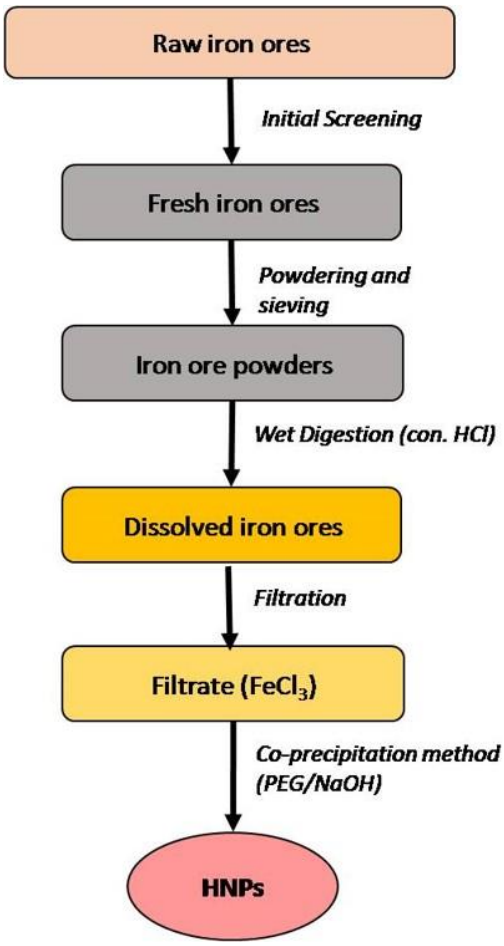

Fig. 3: *Process flow diagram showing the laboratory preparation route of HNPs*

peaks with the major peaks of different iron phases (Fig. 4a). Therefore, the Buttala iron ores are mainly composed of magnetite, goethite, and hematite with trace amounts of spinel and ilmenite.

Results from the chemical analysis revealed that the raw iron ores are mainly composed of Fe_2O_3 (77.80%) with minor concentrations of Al_2O_3, SiO_2, MgO and TiO_2. Here, spinal and quartz may act as the major sources that may contribute to the amount of Al and Si of the iron ore deposit respectively. Also, ilmenite may provide titanium binding with iron and oxygen. According to both XRD and XRF analyses, the Buttala iron ore deposit is a high-grade iron ore deposit with minor quantities of spinal, quartz and ilmenite, which will supply the highest iron content for the manufacturing processes of HNPs in Sri Lanka.

3.2 Mineral and chemical characteristics of AIR

The acid digestion of iron ores is yielded 9.2 wt. % of AIR. It primarily showed characteristic peaks only for spinel, ilmenite and quartz with XRD analysis, clearly indicating the disappearance of the peaks of magnetite, hematite and goethite during the wet digestion (Fig. 4b). The iron-containing minerals in the deposit such as magnetite, hematite and goethite can easily dissolve in concentrated HCl. Therefore, no peaks were observed in this XRD analysis for these iron-bearing minerals. However, other gangue minerals such as spinel, ilmenite and quartz did not dissolve in HCl (11.55M) under 80˚C. Digestion of these minerals can be achieved under higher concentrations of acids and temperature conditions than the conditions used in this study, and through other expensive and time consuming techniques (Mahmoud et al., 2004; Gireesh et al., 2015; Yang et al., 2018).

3.3 Mineralogical and morphological characteristics of prepared HNPs

Fig. 5 shows the XRD pattern of the resulted HNPs. The pattern consists of narrow peaks, indicating the fine nature and small crystallite size of the particles. The peaks at d values of 3.25Å (D_{112}), 2.81Å (D_{031}), 1.99Å (D_{042}) and 1.41Å (D_{323}) (peaks marked as 'ε' in the XRD pattern), correspond to (major phase orthorhombic structure, space group-Pna21) moderate crystalline of ε-Fe_2O_3 (Tuček *et al.*, 2010; Gich *et al.*, 2006). The peaks observed at d-values of 1.69 Å (D_{116}), 1.63Å (D_{211}), and 1.26Å (D_{220}) (peaks marked as 'α' in the XRD pattern) correspond to α-Fe_2O_3 (minor phase trigonal-hexagonal axes structure, space group-R-3c). The ε-Fe_2O_3, ferric oxide phase is a rare metastable polymorph and structurally considered to be an intermediate between hematite α-Fe_2O_3 and maghemite γ-Fe_2O_3 (Dejoie *et al.*, 2014). The main reason for forming different Fe_2O_3 phases could be the mechanism and thermal stability (Nikolic et al., 2017). Due to the metastable nature, the ε-Fe_2O_3 phase is difficult to form and can only be synthesized as nanoscale materials such as nanoparticles, nanowires, and thin films (Machala et al., 2011; Dejoie et al., 2014). The primary reason for this is associated with its low surface energy, which means that properties of surface have a profound influence on the formation and existence of ε-Fe_2O_3 (Machala et al., 2011). Most of these synthesis methods use the γ-Fe_2O_3→ε-Fe_2O_3→α-Fe_2O_3 phase transformation pathway.

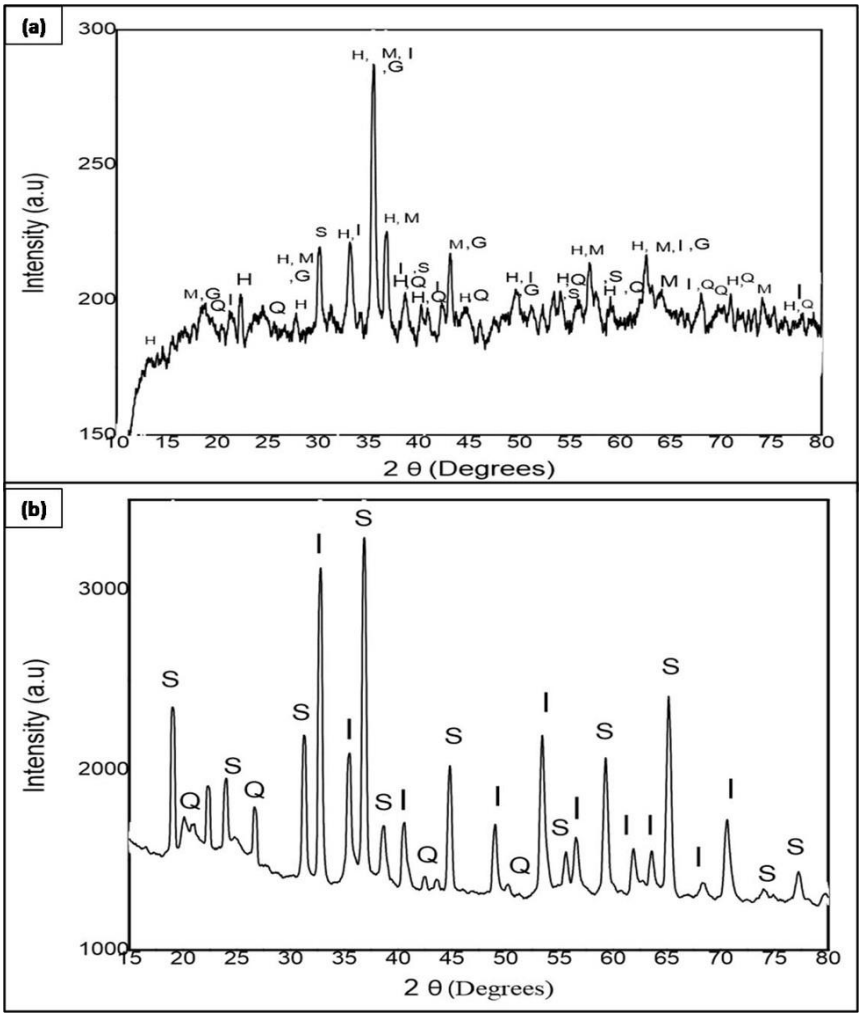

Fig. 4: *The XRD patterns of; (a) raw iron ore and (b) acid insoluble residue, (M-magnetite, H-hematite, G-goethite, S-spinel, I-ilmenite, Q-quartz)*

In this study, mainly ε-Fe_2O_3 and minor α-Fe_2O_3 were formed. The co-precipitation method, which used for this study, previously has been used for magnetite nanoparticles preparation from iron-containing waste ore tailing (Giri et al., 2011). However, by changing conditions such as temperature, pH, rate of addition of NaOH and N_2 gas pressure, the co-precipitation method can be applied for the synthesis of HNPs as it is the cheapest and simplest process compared to other methods to produce spherical shape HNPs from natural ore deposit (Jalil et al., 2019).

At pH ~11.0 and 70 ºC with a low supply of N_2 gas provides suitable conditions to form ε-Fe_2O_3 and α-Fe_2O_3 more than magnetite. Lower N_2 pressure (100 kPa) gas and slow addition (1 ml drop per minute) of NaOH cause oxidation of formed magnetite nanoparticles to γ-Fe_2O_3 →ε-Fe_2O_3→ α-Fe_2O_3 (Mascolo et al., 2013) by reacting with more oxygen in the environment. However, calcination at 200-300 ºC showed a ε-Fe_2O_3/ α-Fe_2O_3 mixture. Normally pure α-Fe_2O_3 nanoparticles form after 400 ºC (Machala et al., 2011).

According to the particle size analyses based on the XRD, it is revealed that the particle size of HNPs ranging from 90 to 130 nm. The particle size analyses based on the SEM images was further confirmed the particle size based on the XRD pattern (Fig. 6). Also, the SEM analyses indicated that the majority of HNPs are in spherical shape while a lesser amount shows irregular flake-like morphology (Fig. 6).

3.4 Industrial aspects of HNPs production using the proposed method

The present study of synthesizing HNPs using the co-precipitation method had given 92.57% maximum yield by showing it as the best

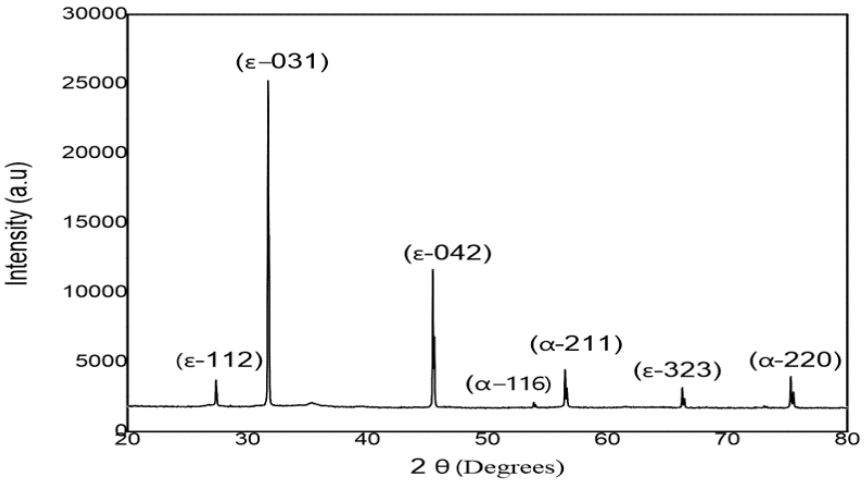

Fig. 5: *The XRD pattern of the synthesized HNPs*

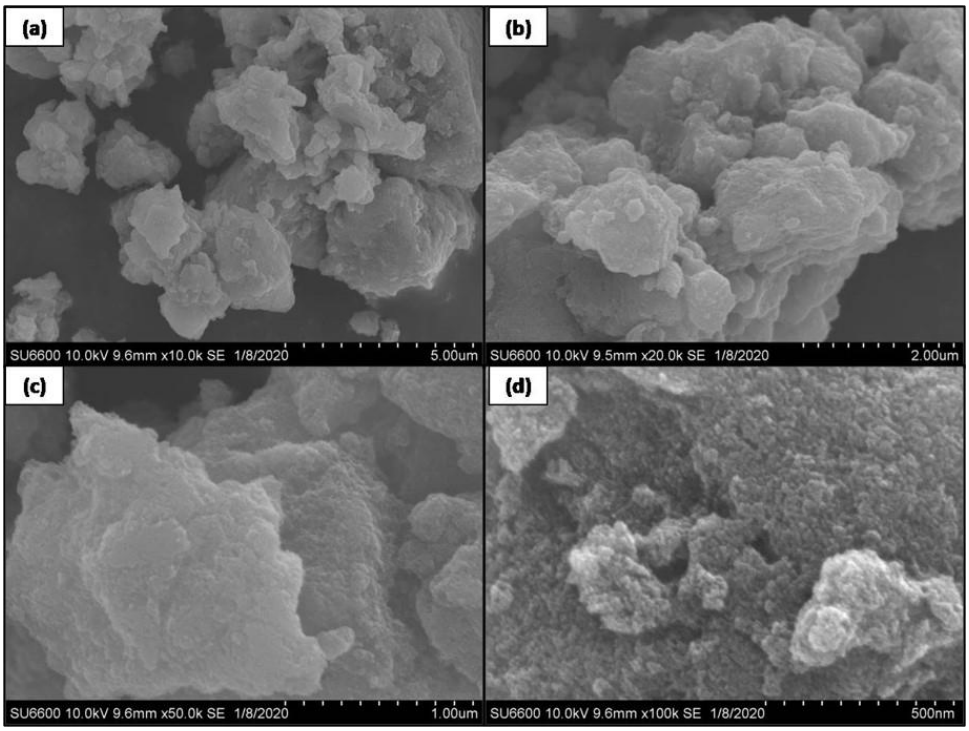

Fig. 6: *(a), (b) & (c) SEM images of irregular flake like HNPs with strong agglomeration and (d) SEM image of spherical shape HNPs with a little agglomeration*

method that can be used industrially when comparing with other chemical synthesizing methods mentioned in previous works of literature (Tuček et al., 2010).

The method being introduced here industrially most viable to prepare ε-Fe_2O_3 than α-Fe_2O_3 that can only be synthesized in laboratory scale (Machala et al., 2011; Campos et al., 2015). Further enhancing this study, with calcination temperature control, only ε-Fe_2O_3 or α-Fe_2O_3 nanoparticles can be obtained separately. As an advantage of utilizing this method for the synthesis HNPs, it was not influenced by the magnetite or maghemite impurities at the end product of the process and it is feasible to extract only the HNPs. Moreover, ilmenite, spinel, and quartz remaining as impurities in the raw iron ores can be processed to be used in other local industry such as glassmaking, production of electronic devices, refractory bricks, jewellery, and sharpening tools, etc. (Nasyrov et al., 2016; Alassi et al., 2017).

4. CONCLUSIONS

The prepared HNPs contain a mixture of ε-Fe_2O_3 / α-Fe_2O_3 nanoparticles of 90-130 nm particle size range. The majority of HNPs shows a spherical shape while a lesser amount shows irregular flake-like morphology. The yield of prepared HNPs is 92.57%. Therefore, the iron ores can be potentially used as a source of iron for the production of HNPs. Studies on possible synthesis of different phases of iron oxide nanoparticles, including magnetite by using the Buttala iron ore deposit as the major source by controlling the process parameters would be advantageous for further economic scale productions.

REFERENCES

Alassi, A., Benammar, M. and Brett, D. (2017). Quartz crystal microbalance electronic interfacing systems. A review, Sensors, 17 (12): pp. 1–41.

Amarasekara, H.M., Sajirupan, S., Senanayake, I.P., Sirisoma, R.H.A.N.C., Chaminda, S.P., Rohitha, L.P.S., Welideniya, H.S. and Abeysinghe, A.M.K.B., (2014). Designing suitable mining method and processing plant for Kukurampola magnetite ore body.

Campos, E. A., Villela, D., Stockler, B., Irineu, J., Oliveira, S., Mattos, C., Cássia, R. D. and Dutra, L. (2015). Synthesis , Characterization and Applications of Iron Oxide Nanoparticles – a Short Review, 7: pp. 267–276.

Chen, J., Xu, L., Li, W. and Gou, X. (2005). α-Fe_2O_3 nanotubes in gas sensor and lithium-ion battery applications, journal of Advanced Materials, 17(5), pp. 582–586.

Chen, J., Macfarlane, S., Zhang, C., Yu, K. and Zhou, W. (2017). Chemistry of Hydrolysis of $FeCl_3$ in the Presence of Phosphate to Form Hematite Nanotubes and Nanorings.Crystal Growth & Design. Published by American Chemical Society, pp.1-11.

Cooray, P.G., 1984. An introduction to geology of Sri Lanka (Ceylon). 2nd revised ed. Colombo; National Museum Department. pp.81-83, 211-212.

Dejoie, C., Sciau, P., Li, W., Noe, L., Mehta, A., Chen, K., Luo, H., Kunz, M., Tamura, N.& Liu, Z. (2014. Learning from the past: Rare ε-Fe_2O_3 in the ancient black-glazed Jian (Tenmoku) wares, Tech. report, 4, 1–9.

Díaz, L. M., Montalvo, G. G., Valiente, M. M. and Martínez, O. S. A. (2016). Study and characterization of the micellar phase of the polyethylene glycol 40 stearate, water, and soy lecithin system, Journal of Revista de la Academia Colombiana de Ciencias Exactas, Físicas y Naturales, 40 (156): p. 412.

Dissanayake, D. M. S. N., Mantilaka, M. M. M. G. P. G., Palihawadana,T. C., Chandrakumara, G. T. D., Silva, R. T. D., Pitawala, H. M. T. G. A., Silva, K. M.N.D. and Amaratunga, G. A. J. (2019). Facile and low-cost synthesis of pure hematite (α-Fe_2O_3) nanoparticles from naturally occurring laterites and their superior adsorption capability towards acid-dyes. Journal of Royal Society of Chemistry: 21249–21257.

Fernando, L. J. (1986). Mineral resources of Sri Lanka, Natural Resources, energy and science Authority, 47/5, Maitland Place, Colombo 7.

Francis, M. A. B. F., Annie, J. and Varma, P. R. H. (2010). Nano iron oxide – hydroxyapatite composite ceramics with enhanced radiopacity, Journal of mater sci: mater med: 1427–1434.

Gich, M., Frontera, C., Roig, A., Taboada,E., Molins, E., Rechenberg, H. R., Ardisson, J. D., Macedo,W. A. A., Ritter,C., Hardy,V., Sort,J., Skumryev,V. and Nogues, J.(2006). High- and low-temperature crystal and magnetic structures of ε-Fe_2O_3 and their correlation to its magnetic properties, Chemistry of Materials, American Chemical Society, 18(16): 3889–3897.

Gireesh, V. S., Vinod, V. P., Krishnan, N. S. and Ninan, G. (2015). Catalytic leaching of ilmenite using hydrochloric acid: A kinetic approach, International Journal of Mineral Processing, 134: 36–40.

Giri, S. K., Das, N. N. and Pradhan, G. C. (2011). Synthesis and characterization of magnetite nanoparticles using waste iron ore tailings for adsorptive removal of dyes from aqueous solution, Journal of Colloids and Surfaces A: Physicochemical and Engineering Aspects. 389(1–3): 43–49.

Herath, M.M.J.W., 1995. Economic geology Sri Lanka: Fifth edition, Ministry of Industrial Development, Colombo. pp.60-70.

Hewathilake, H. P. T. S., Cooray, J. T. and Silva, S. N. De (2013). Magnetometer Characterization of Iron Ore Deposit in Buttala , Sri Lanka, Proceedings to 29th Technical Sessions of Geological Society of Sri Lanka, pp. 17–20.

Hua, J. and Gengsheng, J. (2009). Hydrothermal synthesis and characterization of monodisperse α-Fe_2O_3 nanoparticles, Journal of Materials, 63(30): 2725–2727.

Jalil, Z.,Rahwanto, A., Mulana, F., and Handoko, E.(2019). Synthesis of nano-hematite (Fe_2O_3) extracted from natural iron ore prepared by mechanical alloying method. AIP Conference Proceedings 2151, 020041(1-5).

Jayawardena, D. (1984). The present status of the development of mineral resources in Sri Lanka, Journal of the National Science Foundation of Sri Lanka, 12(1): p. 53.

Jayawardana, D. T., Balasooriya, N.W.B, and Weerakoon, P. (2014) Geochemical Characteristics of Hydrated Iron-Ore Deposit in Dela , Sri Lanka, Journal of Geological Society of Sri Lanka (16), pp.43-52

Lassoued, A., Dkhil, B., Gadri, A. and Ammar, S. (2017). Control of the shape and size of iron oxide (α-Fe_2O_3) nanoparticles synthesized through the chemical precipitation method. Journal of Results in Physics, pp. 3007–3015.

Lin, C.C. and Chen, Y.H. (2014). Effect of nano-hematite morphology on photocatalytic activity. Journal of Phys Chem Minerals,:014-0686-9.

Liu, H., Guo, H., Li, P. and Wei, Y. (2008) The transformation of ferrihydrite in the presence of trace Fe(II): The effect of the anionic media.Journal of Solid State Chemistry, 181(10): 2666–2671.

Liu, H., Wei, Y. and Sun, Y. (2005) The Formation of hematite from ferrihydrite using Fe(II) as a catalyst, Journal of Molecular Catalysis A: Chemical, 226(1): 135–140.

Lu, J., Chen, D. and Jiao, X. (2006). Fabrication, characterization, and formation mechanism of hollow spindle-like hematite via a solvothermal process. Journal of Colloid and Interface Science, 303: 437–443.

Machala, L., Tuček, J. and Zbořil, R. (2011). Polymorphous transformations of nanometric iron(III) oxide: A review', Chemistry of Materials, 23(14): 3255–3272.

Mahmoud, M. H. H., Afifi, A. A. I. and Ibrahim, I. A. (2004). Reductive leaching of ilmenite ore in hydrochloric acid for preparation of synthetic rutile, Journal of Hydrometallurgy, 73(1–2): 99–109.

Manjula, H.A.K.L and Madugalla T.B.N.S., (2018). Mineral and chemical characterization of iron ore deposit in Buttala, Sri Lanka: implication for its economic potential,7th Annual Science Research Sessions,Faculty of Applied Sciences, South Eastern university of Sri Lanka, ASRS 2018, p. 22.

Manjula, H. A. K. L., Marambe, M. K. A. Y. A. and Madugalla, T. B. N. S. (2020). Economic Appraisal of Iron Ore Deposit in Buttala , Sri Lanka : Preliminary Mineral And Chemical Evidences, Journal of Geological Society of Sri Lanka. 21(1): 47–55.

Mascolo, M. C., Pei, Y. and Ring, T. A. (2013). Room Temperature Co-Precipitation Synthesis of Magnetite Nanoparticles in a Large ph Window with Different Bases, Journal of Materials, 6(12): 5549–5567.

Meng, X., Qin, G., Goddard, W. A., Li, S., Pan, H., Wen, X., Qin, Y. and Zuo, L. (2013). Theoretical Understanding of Enhanced Photoelectrochemical Catalytic Activity of Sn-Doped Hematite : Anisotropic Catalysis and Effects of Morin Transition and Sn Doping. Journal of Physical Chemistry, 117: 3779−3784.

Müller, M., Carlo, J., Quadros, F., Dalpasquale, M., Zvolinski, M., Fernando, M., Huila, G. and Jac, F. (2015). 'Dyes and Pigments Synthesis and characterization of iron oxide pigments through the method of the forced hydrolysis of inorganic salts, Journal of Dyes and Pigments, 120(3): 271-278.

Nasyrov, R. S., Lopatin, V. M. and Lunin, B. S. (2016). Internal Friction in Quartz Glass Made Using Natural and Synthetic Raw Material, Journal of Glass and Ceramics, 72(11–12): 437–440.

Nikolic, V. N., Spasojevica, V., Panjanb, M., Kopanja, L., Mrakovica, A. and Tadica, M. (2017). Re-formation of metastable ε-Fe_2O_3 in post-annealing of Fe_2O_3/SiO_2 nanostructure: Synthesis, computational particle shape analysis in micrographs and magnetic properties, Journal of Ceramics International. 43(10): 7497–7507.

Panda, A. K., Sarkar, G. and Manna, K. (2009). Physicochemical studies on surfactant aggregation 1. Effect of polyethylene glycols on the micellization of SDS, Journal of Dispersion Science and Technology, 30(8): 1152–1160.

Schwertmann, U., Friedl, J. and Stanjek, H. (1999). From Fe (III) Ions to Ferrihydrite and then to Hematite, Journal of colloid and Interface Science, 209: 215–223.

Senaratne, A. and Fernando, G. W. A. (2001). Discovery of a new primary magnetite deposit in Wellawaya, Sri Lanka. The Annual Research Sessions, University of Peradeniya. Sri Lanka. 6, p. 133.

Sultan, S., Kareem, K. and He, L. (2016). Surface & Coatings Technology Synthesis , characterization and resistant performance of α-Fe_2O_3/SiO_2 composite as pigment protective coatings, Journal of Surface & Coatings Technology, 300: 42–49.

Tadic, M., Panjan, M.,Damnjanovic, V. and Milosevic. I. (2014). Magnetic properties of hematite (α-Fe_2O_3) nanoparticles prepared by hydrothermal synthesis method, Journal of Applied Surface Science, 320: 183–187

Tang, B., Wang, G., Zhuo, L., Ge, J. and Cui, L. (2006). Facile route to α -FeOOH and α -Fe_2O_3 nanorods and magnetic property of α-Fe_2O_3 nanorods, Journal of Inorganic Chemistry, 45: 5196–5200.

Tuček, J. Zboril, R., Namai, A., and Ohkoshi, S. (2010). ε-Fe_2O_3: An advanced nanomaterial exhibiting giant coercive field, millimeter-wave ferromagnetic resonance, and magnetoelectric coupling, Journal of Chemistry of Materials, 22(24): 6483–6505.

Wang, H., Beermann, N., Vayssieres, L., Hagfeldt, A., Lindquist, S., (2002). Aqueous photoelectrochemistry of hematite nanorod array, Journal of Solar Energy Materials & Solar Cells, 71: 231–243.

Wheeler, D. A., Wang, G., Ling, Y., Li, Y., Zhang, J. Z. (2012). Environmental Science dynamics , and photoelectrochemical properties, Journal of Royal Society of Chemistry: 6682–6702.

Wu, W., Xiao, X.H., Zhang, S.F., Zhou, J., Fan, L.X., Ren, F. and Jiang, C.Z. (2010). Large-scale and controlled synthesis of iron oxide magnetic short nanotubes: shape evolution, growth mechanism, and magnetic properties. Journal of Physical Chemistry, 114: 16092–16103.

Yang, Y. A, H., Zhuang, J. and Wang, X. (2011). Morpholoy-Controlled Synthesis of Hematite Nanocrystals and Their Facet Effects on Gas-Sensing Properties, Journal of Inorganic Chemistry, 10143–10151.

Yang, C., Li, S., Bai, J. and Han, S. (2018). Advanced purification of industrial quartz using calcination pretreatment combined with ultrasound-assisted leaching. Journal of Acta Geodyn. Geomater. 15(2): 187–195.

Yasuhara, A., Ai, H. and Hochella, M. F. (2019). Mn(II)oxidation catalyzed by nanohematite surfaces and manganite / hausmannite core-shell nanowire formation by self-catalytic reaction, Journal of Geochimica et Cosmochimica Acta, 258: 79–96.